

# Water-gas shift: steady state isotope switching study of the water-gas shift reaction over Pt/ceria using *in-situ* DRIFTS

Gary Jacobs\*, Adam C. Crawford, and Burtron H. Davis

Center for Applied Energy Research, University of Kentucky, 2540 Research Park Drive, Lexington, KY 40511

Received 28 September 2004; accepted 02 December 2004

The stability of surface formates generated by reaction of bridging OH groups with CO is an important first criterion supporting the idea that the rate limiting step of WGS involves formate decomposition. The second important factor is that, in the presence of water, shown directly by the measurements obtained during this steady state isotope switching study, the forward decomposition of surface formates to CO<sub>2</sub> and H<sub>2</sub> is strongly auto-catalyzed by H<sub>2</sub>O, in agreement with the findings of Shido and Iwasawa. Based on a normal kinetic isotope effect previously observed with H<sub>2</sub>O:D<sub>2</sub>O switching and the response of surface formate coverages to the WGS rate under steady state conditions when a high H<sub>2</sub>O:CO ratio is employed, the conclusion is drawn that a surface formate mechanism is likely operating for the low temperature water gas shift reaction.

**KEY WORDS:** platinum; Pt; ceria; CeO<sub>2</sub>; vacancies; water-gas shift; LTS; isotope exchange; DRIFTS; bridging OH groups.

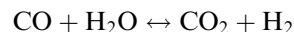
## 1. Introduction

The water-gas shift (WGS) reaction is being extensively studied for the production of H<sub>2</sub> from the steam reforming and partial oxidation of hydrocarbons [1–5]. One potential WGS reactor configuration involves staged high temperature shift (HTS) and low temperature shift (LTS) catalytic reactors. This is a direct consequence of the thermodynamic limitations regarding equilibrium conversion of CO associated with the exothermic nature of WGS. The WGS system would be used primarily to convert CO, which is a poison for fuel cell electrode catalysts; in the process, especially for the HTS section, more H<sub>2</sub> would be produced. Recent investigations focus on the potential that metal promoted partially reducible oxide catalysts (e.g., ceria) may offer for catalyzing the more difficult LTS reaction. While from a thermodynamic standpoint the equilibrium conversion is high at low temperatures, the kinetics are unfavorable. Therefore, advanced WGS catalysts operating in the low temperature range are in demand, and catalysts such as Pt/ceria appear to offer promise.

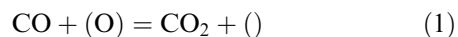
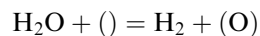
The heterogeneous WGS reaction has been commercialized and can be categorized into two different processes, depending on the catalyst employed. The HTS process uses an iron-chromia-based catalyst, and is operated at temperatures of about 320–450 °C. The LTS process uses either copper-based catalyst or sulfided molybdenum-based catalyst, and normally is operated at 200–250 °C.

The chemical equilibrium constant of the WGS reaction is significantly dependent on the reaction tem-

perature. At 200 °C,  $K_p$  is 228 but at 400 °C it is only 11.8, illustrating the thermodynamic limitations imposed by high operating temperatures.



A range of mechanisms for the heterogeneous WGS reaction have been proposed and disagreement exists about the elementary steps of the reaction. The debate centers around the reaction involving the oxidation-reduction mechanism proposed by Temkin *et al.* [6,7], a mechanism proposed by Nakanishi and Tamaru [8], a Rideal–Eley-type mechanism [9] or a Langmuir–Hinshelwood-type mechanism [10]. At one extreme is the “redox” mechanism [6,7] that involves reduction and oxidation steps in the mechanism. It may be represented by the following reactions:

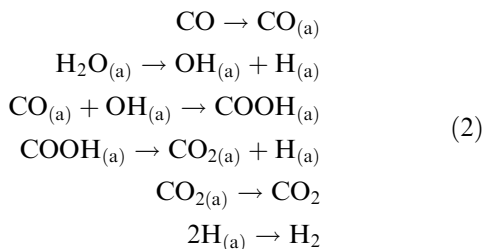
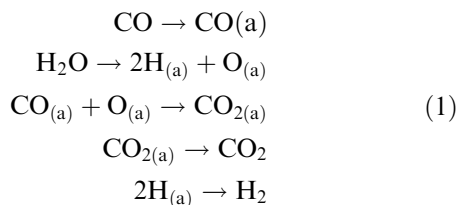


Here (O) is an oxygen atom on the catalyst (typically iron oxide) surface and () is a vacant site on the surface caused by the removal of an oxygen atom. The WGS reaction proceeds via alternate oxidation and reduction steps on the partially reduced surface of the oxide. The early support for this mechanism came from kinetic data. Temkin and coworkers used this mechanism to derive several kinetic rate expressions and their experimental data were in good agreement with the derived rate expressions. They considered the agreement to be strong evidence for the redox mechanism.

Oki *et al.* [11–17] applied the stoichiometric number method, developed by Horiuto [18,19]. By measuring the stoichiometric number for the elementary steps, they

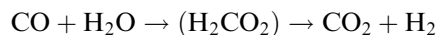
\*To whom correspondence should be addressed.

proposed the following two possible mechanisms for the heterogeneous WGS reaction over an iron oxide catalyst:



where subscript (a) represents a surface-adsorbed species. In their mechanisms, as the initial steps, carbon monoxide is nondissociatively adsorbed on the surface while water is dissociatively adsorbed on the surface. The reaction evolves by interaction between two neighboring surface species. The final products are produced by desorption of surface species. The second mechanism involves a surface formate species whereas the first mechanism does not. Their studies suggest that adsorption of CO is the rate controlling step in the initial stage of the reaction but the desorption of surface hydrogen becomes more dominant as the reaction approaches equilibrium.

Hervijnen and de Jong [20,21] made kinetic studies of the WGS reaction using Cu–ZnO catalysts. They suggested that the reaction proceeds via a formate-type intermediate on the catalyst surface, and may be shown as:



They described the kinetics by a Langmuir-Hinshelwood type equation of the following form:

$$\begin{aligned}
 r = & kP_{\text{CO}}P_{\text{H}_2\text{O}} / 1 + K_{\text{H}_2\text{CO}_2}P_{\text{CO}}P_{\text{H}_2\text{O}} + K_{\text{CO}}P_{\text{CO}} \\
 & + K_{\text{H}_2\text{O}}P_{\text{H}_2\text{O}}
 \end{aligned}$$

where  $r$  is the reaction rate,  $P_{\text{CO}}, P_{\text{H}_2\text{O}}$  are the pressure of CO and  $\text{H}_2\text{O}$ ,  $k$  is the rate constant and  $K_{\text{H}_2\text{CO}_2}, K_{\text{CO}}, K_{\text{H}_2\text{O}}$  are the surface coverage parameters for  $\text{H}_2\text{CO}_2$ , CO and  $\text{H}_2\text{O}$ , respectively. They investigated the decomposition of formic acid on the same catalyst and found that the decomposition proceeded through the formate-like intermediate. The rate of the formic acid decomposition is similar to that of the forward WGS reaction and has the same temperature dependence. The ratio of the CO/ $\text{CO}_2$  products is the same as the ratios of the forward and reverse shift reactions at

equilibrium. They conclude that the decomposition of a pseudo-stable formate-type intermediate is the rate determining step in the WGS reaction over the Cu/ZnO catalyst. FTIR spectroscopy studies support the existence of the adsorbed formate species on the catalyst surface [22].

In reviewing the early work using isotopic tracers in stoichiometric number investigations, it was concluded that the data permitted the elimination of some mechanisms, such as the Temkin oxidation-reduction mechanism, widely accepted at one time [23]. Likewise a Rideal–Eley-type and a Langmuir–Hinshelwood-type mechanism are not consistent with a stoichiometric number of 2. The view at the time of the review, it seemed that the rate-controlling step probably changed as the reaction approached equilibrium, thereby complicating the situation appreciably.

Significant data obtained following this review by Raje and Davis have been considered to support the redox mechanism [e.g., 24–28]. Other studies, emphasizing IR and isotope tracer data, favored the formate mechanism [29–36]. Recently, Tibiletti *et al.* [37] indicate that *in operando* studies are necessary to investigate the true reactivity pattern of surface species during the reverse WGS (RWGS) over noble metal-promoted ceria. Formates were identified as the most reactive surface intermediates under an inert gas but they exchanged significantly slower than the other surface species under RWGS reaction conditions in the isotopic exchange experiment. Tibiletti *et al.* [37] therefore concluded that the surface formates are spectator species.

The present study was undertaken to utilize isotopic switching of  $^{12}\text{CO}$  to  $^{13}\text{CO}$  *in operando* studies under the conditions utilizing high  $\text{H}_2\text{O}/\text{CO}$  ratios appropriate for the low-temperature WGS (LT-WGS) reaction to convert most of the CO remaining from high-temperature WGS. These ratios differ from those utilized by supporters of the redox mechanism but they are typical of the conditions following the HT-WGS stage of a fuel cell processor.

## 2. Experimental

### 2.1. Catalyst preparation

High surface area samples ceria were prepared via homogeneous precipitation of the nitrate in urea with aqueous ammonia in a similar manner to Li *et al.* [27]. The idea is an adaptation of work conducted on CuO–ZrO<sub>2</sub> methanol synthesis catalysts [38], whereby urea decomposition is a slow process resulting in a slower, more homogeneous precipitation. On a basis of 30 g CeO<sub>2</sub>, an appropriate amount of Ce(NO<sub>3</sub>)<sub>3</sub>·6H<sub>2</sub>O (Alfa Aesar, 99.5%) and 240 g urea (Alfa Aesar, 99.5%) were dissolved in 900 mL of deionized water, and to the solution about 30 mL NH<sub>4</sub>OH (Alfa Aesar, 28–30%

NH<sub>3</sub>) was added dropwise (~1 mL/min). The mixture was then boiled at 100 °C with constant stirring. The precipitate was filtered, washed with 600 mL of boiling deionized water, and dried in an oven (100 °C) overnight. The dried precipitate was then crushed and calcined in a muffle furnace at 400 °C for 4 h.

BET surface area of the ceria was 105 m<sup>2</sup>/g. Platinum was added via incipient wetness impregnation with tetraammine platinum (II) nitrate solution. The catalyst was calcined at 400 °C for 4 h after metal component addition.

## 2.2. BET surface area

BET Surface Area measurements were carried out in a Micromeritics Tristar 3000 gas adsorption analyzer. In each trial, a weight of approximately 0.25 g of sample was used. The adsorptive gas was nitrogen (N<sub>2</sub>) and the adsorption was carried out at the boiling temperature of liquid nitrogen.

## 2.3. Diffuse reflectance infrared fourier transform spectroscopy (DRIFTS)

A Nicolet Nexus 870 was used, equipped with a DTGS-TEC detector. A high pressure/high temperature chamber fitted with ZnSe windows was utilized as the WGS reactor for *in-situ* reaction measurements. The gas lines leading to and from the reactor were heat traced, insulated with ceramic fiber tape, and further covered with general purpose insulating wrap. Scans were taken at a resolution of four to give a data spacing of 1.928 cm<sup>-1</sup>. Typically, 32–128 scans were taken to improve the signal to noise ratio. The sample utilized was 33 mg of catalyst.

A steam generator consisted of a downflow tube packed with quartz beads and quartz wool heated by a ceramic oven and equipped with an internal thermocouple. The lines after the steam addition were heat traced. The steam generator and lines were run at the same temperature as that at the *in-situ* sample holder of the DRIFTS cell. This allowed us to accurately bring the reactants to the desired reaction temperature. Water was added to the steam generator by a thin needle welded to a 1.6 mm line. A precision ISCO Model 500D syringe pumps was used to feed the water and deuterated water.

Feed gases flow rates were controlled by Brooks 5850 series E mass flow controllers. A selector switch was

placed on the CO line prior to the mass flow controller and the dead volume minimized. The pressure of the CO tanks were set at a low enough pressure to minimize transport time, but high enough to give an accurate flow through the flow controller.

## 3. Results and discussion

### 3.1. Standard characterization

BET surface areas and porosity parameters of ceria and Pt/ceria are included in Table 1. Addition of urea to the preparation procedure has allowed us to double the surface area of ceria over standard precipitation using ammonium hydroxide. Previous XRD measurements have indicated that the domain size of the ceria was approximately 8.4 nm. TPR profiles have been reported before (e.g., see [32,33]). In comparing reduction profiles of sintered ceria and high surface area ceria, the bulk ceria is assigned to reduction at close to 750 °C. Reduction of the surface shell of ceria, present as a large broad peak on the high surface area ceria support, occurred between 400 and 500 °C. Pt catalyzed and therefore shifted the peak for the reduction of the surface shell of ceria to lower temperatures (approximately 250 °C), but had little effect on the bulk reduction. We have conducted XANES experiments [33] which directly measure the extent of the partial reduction of ceria, not reproduced here, which support the above conclusions. After reduction, which involved decomposition of surface carbonates, DRIFTS indicated that bridging OH groups were clearly produced on the surface of ceria [35], a process that is accompanied by a decrease in the oxidation state from +4 to +3 of the Ce surface shell atoms involved.

### 3.2. In-situ DRIFTS experiments

#### 3.2.1. Adsorption of <sup>12</sup>CO and <sup>13</sup>CO

To carry out valid *in-situ* DRIFTS experiments utilizing isotope exchange, it is necessary to obtain appropriate spectra to be used as references. Therefore, after reduction of the catalyst in hydrogen at 300 °C, the catalyst was cooled to 225 °C and purged in N<sub>2</sub> prior to adsorption of CO. Figure 1 indicates that the bridging OH groups (band at ca. 3650 cm<sup>-1</sup> with shoulder at 3675 cm<sup>-1</sup>) react with CO to generate surface formates. When <sup>12</sup>CO is adsorbed, the surface formates are characterized by bands associated with the OCO asymmetric and symmetric vibrations (ca. 1580 and 1300 cm<sup>-1</sup>) and C–H vibrations (ca. 2955 and 2840 cm<sup>-1</sup>). Some carbonate is also evident by bands at 1460 and 1395 cm<sup>-1</sup>, as well as ca. 860 cm<sup>-1</sup>, as previously assigned [39]. The bands involving carbon shift measurably when the <sup>13</sup>C isotope is employed. The bands are similar to previous reports [37].

Table 1  
BET surface area, and porosity results

Description	BET SA (m <sup>2</sup> /g)	Pore Volume (cm <sup>3</sup> /g)	Radius (nm)
Ceria	105.5	0.121	2.29
1%Pt/Ceria	99.6	0.115	2.32

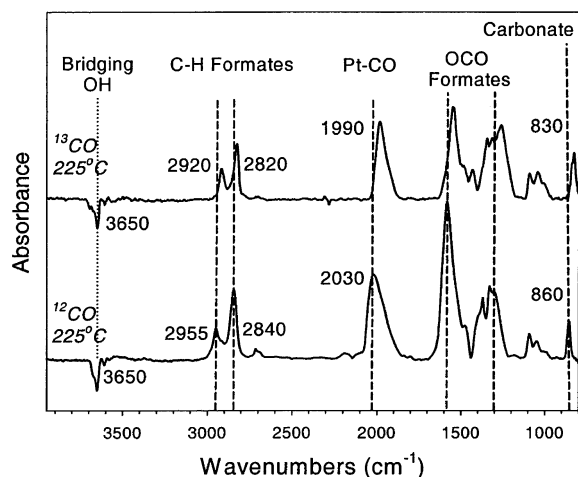


Figure 1. Adsorption of  $^{12}\text{CO}$  (bottom) and  $^{13}\text{CO}$  (top) to Pt/ceria. The catalyst was first reduced in hydrogen (100 ccm) at 300 °C, cooled to 225 °C, and purged in nitrogen. Conditions: 3.75 ccm CO and 135 ccm nitrogen.

### 3.2.2. Transport considerations and isotope surface exchange

To make valid claims regarding whether surface species are possible intermediates, it is first necessary to quantify the exchange rates **in the absence of reaction**. Figures 2a and 3a show how the adsorbed CO surface species respond in the absence of water during the period following the switch from  $^{12}\text{CO}$  to  $^{13}\text{CO}$ . Interestingly, the exchange rate of Pt-CO is very rapid. During a RWGS reaction study led by Tibiletti *et al.* [37], the fast response of Pt-CO during RWGS was used as evidence to support a redox mechanism. However, the fast exchange rate of CO on the surface of Pt is a factor that must first be evaluated.

As expected from the historical perspective, surface formates are remarkably stable on Pt/ceria. Even after 80 min, less than 30% of the formates on the surface had exchanged. Surface carbonates revealed an intermediate, but rather slow exchange rate in comparison with Pt-CO, with 50% of the carbonate exchanging in approximately 1 h.

### 3.2.3. Steady state isotope switching

In contrast to the exchange rates in b above, for the WGS reaction at a high  $\text{H}_2\text{O}/\text{CO}$  ratio, great differences were observed. As shown in figure 2a, while the Pt-CO intensity is little affected, that of the surface formates is significantly attenuated. More importantly, the time required for exchange from  $^{12}\text{C}$ -labeled formate to  $^{13}\text{C}$ -formate dramatically decreases in the presence of water. From a rather stable formate in the absence of water, 50% of the  $^{12}\text{C}$ -formates are enhanced within about 8 min. The exchange rate of the  $\text{CO}_2$  product coincided with the decomposition rate of the formate. However, one cannot by the isotope exchange experiment alone rule out the possibility that Pt participates in the mechanism, as the Pt-CO exchanged at virtually an

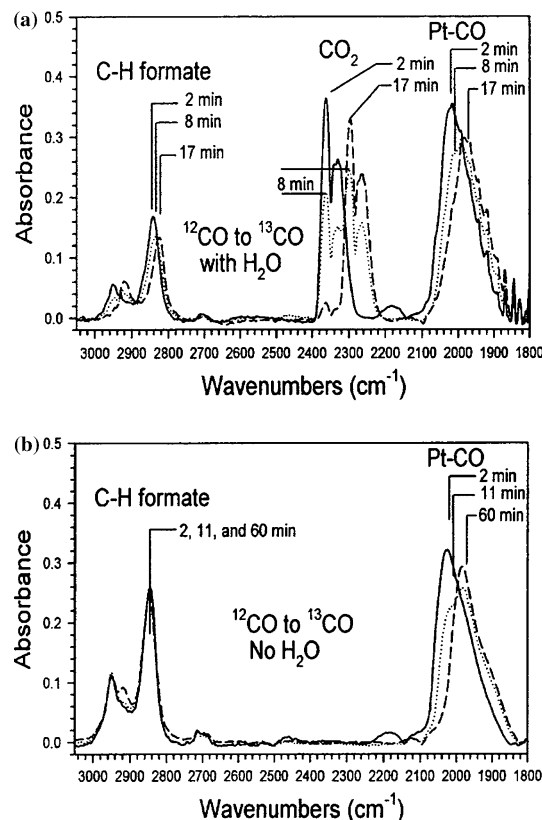


Figure 2. (a) Isotope exchange in the absence of water at 225 °C. The formates are observed to exchange very slowly, while Pt-CO readily exchanges. Conditions: 3.75 ccm CO and 135 ccm nitrogen. (b) The isotope exchange in the presence of water. The formates readily exchange. Their exchange follows the exchange of  $\text{CO}_2$  product. Conditions: 3.75 ccm CO; 125 ccm  $\text{H}_2\text{O}$ ; 10 ccm nitrogen.

identical rate. However, in comparison with the exchange rate in the absence of water, only a small decrease in time needed for exchange was observed. The exchange rate of carbonate also decreased, coinciding within experimental error with that of the formate.

However, not all of the carbonate exchanged and, some residual carbonate ( $\sim 20\%$ ) remains on the catalyst surface, in agreement with our previous *in-situ* DRIFTS findings [31]. As shown in Figure 4, if one considers only the carbonate that exchanges by dividing the carbonate signal by 0.8, the carbonates fall on essentially the same curve as the formate exchange. The exchange time of the dead volume of the system was measured by conducting the switch and following the CO signals in the absence of catalyst (figure 3c).

The findings, we argue, strongly support a formate mechanism that encompasses the observations previously put forth by Shido and Iwasawa [29,30]. That is, in the presence of water, the forward decomposition of surface formates is auto-catalyzed. Considering the exchange time during WGS, unidentate carbonate is also a likely intermediate, and we have previously observed in transient experiments that unidentate carbonate is produced during formate decomposition by water [35].

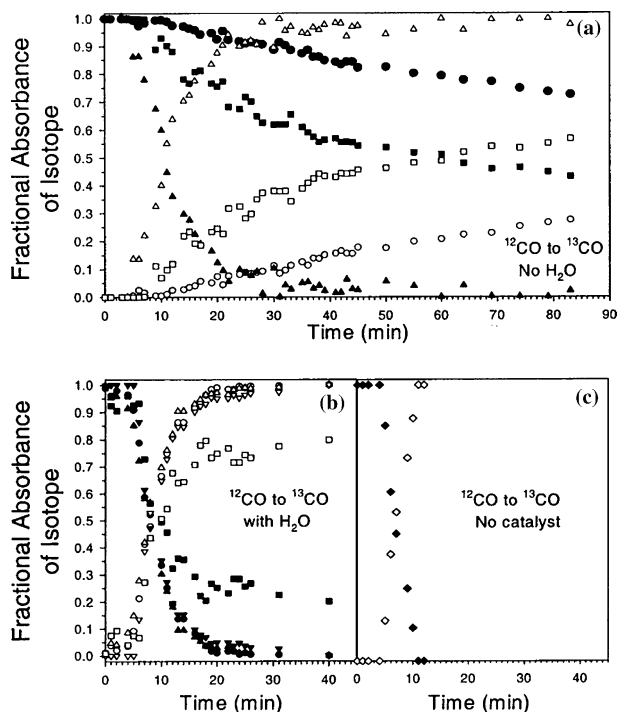


Figure 3. (a) Isotope exchange in the absence of water at 225 °C. The formates are observed to exchange very slowly, while  $\text{Pt-CO}$  readily exchanges. Conditions: 3.75 ccm  $\text{CO}$  and 135 ccm nitrogen. (b) The isotope exchange in the presence of water. The formates and carbonates readily exchange. Their exchange follows the exchange of  $\text{CO}_2$  product. Conditions: 3.75 ccm  $\text{CO}$ : 125 ccm  $\text{H}_2\text{O}$ : 10 ccm nitrogen. (c) Switching in the absence of catalyst to quantify exchange time of the dead volume. Symbols: filled –  $^{12}\text{C}$  containing species; open –  $^{13}\text{C}$  containing species; circles – formates; squares – carbonates; upright triangles –  $\text{Pt-CO}$ ; inverted triangles –  $\text{CO}_2$ ; diamonds (graph C only) –  $\text{CO}$ . Bands followed: formate C–H bands,  $\text{Pt-CO}$ , carbonate ( $860\text{--}830\text{ cm}^{-1}$ ).

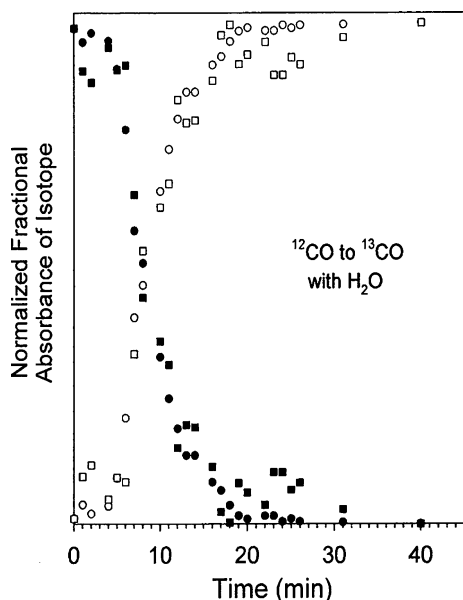
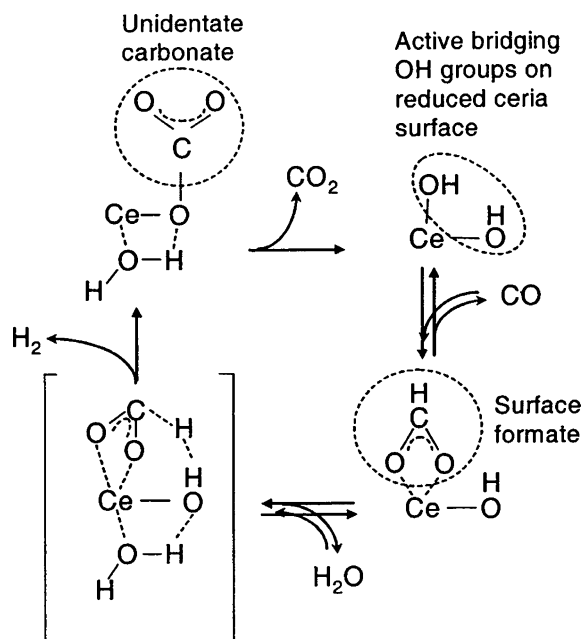


Figure 4. Comparison of the fractional absorbance of the formates and carbonates after normalization of the carbonate. The rates of exchange fall on essentially the same curve.

The results of the present study should be considered for two conditions. Under the nonreaction conditions (without water addition), the exchange rate of the  $^{12}\text{C}$ -labeled carbonate and  $\text{Pt-CO}$  exchange with  $^{13}\text{C}$ -labeled  $\text{CO}$  much more rapidly than that of the  $^{12}\text{C}$ -labeled formate. In contrast, when water is added with the  $^{13}\text{CO}$ , the rate of the exchange with  $^{12}\text{C}$ -labeled carbonate increases from a half-time of about 65 min to about 2.5 min whereas the exchange rate of the  $^{12}\text{C}$ -labeled formate decreases dramatically and becomes essentially equal to that of the carbonate. Thus, the exchange rates observed when only  $\text{CO}$  is added in the gas phase cannot be used to judge the exchange rates obtained when both water and  $\text{CO}$  are added.

A version of the reaction cycle involving a formate intermediate is outlined below [29]:



In this scheme, the formate is converted to produce  $\text{H}_2$  and adsorbed carbonate. If there is no discrimination among the surface carbonate groups, then there should be an exchange of the carbonate with each exchange with the formate group, and this is experimentally observed. Not only does the exchange rate of the carbonate and formate groups become essentially the same, the rate of exchange of both increase dramatically. Thus, in the absence of water, the exchange of carbonate is faster than the formate but when water is present they both increase, to a different extent, to become essentially equal. The results of this study suggest that the observations of Tibiletti *et al.* should be different in the presence of water since the WGS and the RWGS reactions should have a common reaction pathway.

#### 4. Conclusions

Surface formates generated by reaction of bridging OH groups with  $\text{CO}$  are quite stable under low tem-

perature conditions. However, in the presence of water, the forward decomposition of surface formates to  $\text{H}_2$  and  $\text{CO}_2$  is strongly auto-catalyzed. Based upon the observations made in this steady state isotopic switching study, in conjunction with the normal kinetic isotope effect previously observed – and in considering the response of surface formate coverages under WGS conditions – we conclude that a surface formate mechanism is likely operating for the low temperature water gas shift reaction, in agreement with the findings of Shido and Iwasawa. The role of vacancies is important, however, in that they are related to the bridging OH groups. That is, through these dissociation of water on ceria vacancies or the dissociation and spillover of hydrogen to ceria, bridging OH groups are generated at reduced defect centers, and serve as the catalytically active sites.

### Acknowledgment

The work was supported by the Commonwealth of Kentucky.

### References

- [1] *Fuel Cell Handbook*, 5th ed., US DOE, NETL (2000).
- [2] Fuel Cells for Transportation Program Contractors' Annual Progress Report, US DOE, OAAT (1998).
- [3] D.C. Dayton, M. Ratcliff and R. Bain, Fuel Cell Integration A Study of the Impact of Gas Quality and Impurities, NREL/MP-510-30298 (2001).
- [4] A.F. Ghenciu, Curr. Opin. Solid State Mater. Sci. 6 (2002) 389.
- [5] R. Farrauto, S. Hwang, L. Shore, W. Ruettinger, J. Lampert, T. Giroux, Y. Liu and O. Ilinich, Annu. Rev. Mater. Res. 33 (2003) 1.
- [6] N.V. Kul'kova and M.I. Temkin, Zh. Fiz. Khim. 23 (1949) 695.
- [7] G.G. Shchibrya, N.M. Morozov and M.I. Temkin, Kinet. Catal. 6 (1965) 1057.
- [8] J. Nakanishi and K. Tamaru, Trans. Faraday Soc. 59 (1963) 1470.
- [9] V. Glavachek, M. Marek and M. Korzhinkova, Kinet. Catal. 9 (1968) 1107.
- [10] C. Wagner, Adv. Catal. 21 (1970) 323.
- [11] Y. Kaneko and S. Oki, J. Res. Inst. Catal., Hokkaido Univ. 13 (1965) 55.
- [12] Y. Kaneko and S. Oki, J. Res. Inst. Catal. 13 (1965) 169.
- [13] Y. Kaneko and S. Oki, J. Res. Inst. Catal., Hokkaido Univ. 15 (1967) 185.
- [14] S. Oki, J. Happel, M. Hnatow and Y. Kaneko, Proc. 5th Intern. Congr. Catal., (1973), Vol. 1, pp. 173–183.
- [15] S. Oki and R. Mezaki, J. Phys. Chem. 77 (1973) 447.
- [16] S. Oki and R. Mezaki, J. Phys. Chem. 77 (1973) 1601.
- [17] R. Mezaki and S. Oki, J. Catal. 30 (1973) 488.
- [18] J. Horiuti, J. Res. Inst. Catal., Hokkaido Univ. 1 (1948) 8.
- [19] J. Horiuti and T. Nakamura, Adv. Catal. 17 (1967) 1.
- [20] T.V. Herwijnen and W.A. De Jong, J. Catal. 63 (1980) 83.
- [21] T.V. Herwijnen and W.A. De Jong, J. Catal. 63 (1980) 94.
- [22] F.F. Edwards and G.L. Schrader, J. Phys. Chem. 88 (1984) 5620.
- [23] A. Raje and B.H. Davis, in: *Catalysis*, Vol. 12, ed. J. J. Spring (The Royal Soc. Chem., Cambridge, 1996), pp. 52–131.
- [24] T. Bunluesin, R. Gorte and G. Graham, Appl. Catal. B 15 (1998) 107.
- [25] S. Hilaire, X. Wang, T. Luo, R.J. Gorte and J. Wagner, Appl. Catal. 215 (2001) 271.
- [26] X. Wang and R.J. Gorte, Appl. Catal. A 247 (2003) 157.
- [27] Y. Li, Q. Fu and M. Flytzani-Stephanopoulos, Appl. Catal. B 27 (2000) 179.
- [28] Q. Fu, A. Weber and M. Flytzani-Stephanopoulos, Catal. Lett. 77(1–3) (2001) 87.
- [29] T. Shido and Y. Iwasawa, J. Catal. 141 (1993) 71.
- [30] T. Shido and Y. Iwasawa, J. Catal. 136 (1992) 493.
- [31] G. Jacobs, L. Williams, U. Graham, D. Sparks and B.H. Davis, J. Phys. Chem. B 107(38) 10398.
- [32] G. Jacobs, L. Williams, U. Graham, D. Sparks, G. Thomas and B.H. Davis, Appl. Catal. A 252 (2003) 107.
- [33] G. Jacobs, P.M. Patterson, L. Williams, E. Chenu, D. Sparks, G. Thomas and B.H. Davis, Appl. Catal. A 262 (2004) 177.
- [34] G. Jacobs, A.C. Crawford, L. Williams, P.M. Patterson and B.H. Davis, Appl. Catal. A 267 (2004) 27.
- [35] G. Jacobs, P.M. Patterson, U. Graham, D. Sparks and B.H. Davis, Appl. Catal. 269 (2004) 63.
- [36] G. Jacobs, S. Khalid, P.M. Patterson, D.E. Sparks and B.H. Davis, Appl. Catal. 268 (2004) 255.
- [37] D. Tibiletti, A. Goguet, F.C. Meunier, J.P. Breen and R. Burch, Chem. Commun., 2004(14), 1636.
- [38] Y. Amenomiya, I.T. Ali Emesh, K.W. Oliver, and G. Pleizier, *Proc. 9th International Congress on Catalysis*, Vol. 2 (C1 Chemistry), eds. M.J. Phillips and M. Ternan (Chem. Inst. of Canada, Ottawa, Ontario, Canada 1988), p. 634.
- [39] A. Holmgren, B. Andersson and D. Duprez, Appl. Catal. B 22 (1999) 215.